Iranian Journal of Oil & Gas Science and Technology, Vol. 3 (2014), No. 1, pp. 22-33
http://ijogst.put.ac.ir

An Estimation of Wave Attenuation Factor in Ultrasonic Assisted Gravity Drainage Process

Behnam Keshavarzi, Mohammad Javad Shojaei, Mohammad Hossein Ghazanfari*, and Cyrus Ghotbi

Department of Chemical and Petroleum Engineering, Sharif University of Technology, Tehran, Iran

Received: October 19, 2013; *revised:* November 17, 2013; *accepted:* December 25, 2013

Abstract

It has been proved that ultrasonic energy can considerably increase the amount of oil recovery in an immiscible displacement process. Although many studies have been performed on investigating the roles of ultrasonic waves, based on the best of our knowledge, little attention has been paid to evaluate wave attenuation parameter, which is an important parameter in the determination of the energy delivered to the porous medium. In this study, free fall gravity drainage process is investigated in a glass bead porous medium. Kerosene and Dorud crude oil are used as the wetting phases and air is used as the non-wetting phase. A piston-like displacement model with considering constant capillary pressure and applying Corey type approximation for relative permeabilities of both wetting and non-wetting phases is applied. A pressure term is considered to describe the presence of ultrasonic waves and the attenuation factor of ultrasonic waves is calculated by evaluating the value of external pressure applied to enhance the flow using the history matching of the data in the presence and absence of ultrasonic waves. The results introduce the attenuation factor as an important parameter in the process of ultrasonic assisted gravity drainage. The results show that only a low percentage of the ultrasonic energy (5.8% for Dorud crude oil and 3.3% for kerosene) is delivered to the flow of the fluid; however, a high increase in oil recovery enhancement (15% for Dorud crude oil and 12% for Kerosene) is observed in the experiments. This proves that the ultrasonic waves, even when the contribution is not substantial, can be a significantly efficient method for flow enhancement.

Keywords: Ultrasonic Waves, Gravity Drainage, Attenuation Factor, Glass Bead Pack

1. Introduction

In a pioneering study on the effect of ultrasonic waves on flow behavior, Duhon and Campbell (1965) conducted water-flood tests under ultrasonic exposure and showed that ultrasonic energy caused an improvement in oil recovery. Cheriskiy et al. (1977) described a sharp increase in the permeability of core samples saturated with fresh water in the presence of acoustic field. Beresnev and Johnson (1994) mentioned that the application of elastic waves improved fluid percolation in porous media. Hamida and Babadagli (2007, 2008) studied the capillary interaction and oil recovery during capillary imbibition process under ultrasonic waves and found that ultrasonic irradiation enhanced the capillary imbibition recovery of oil for various fluid pairs, and that the process was dependent on the interfacial tension and density of the fluids. They also stated that ultrasonic enhanced surfactant solubility but reduced surfactant adsorption on the rock matrix. Naderi and Babadagli (2008, 2010) revealed the

* Corresponding Author:
Email: ghazanfari@sharif.edu

positive effect of ultrasonic energy on heavy-oil recovery for rocks with different wettability conditions. They also analyzed the effect of some parameters including ultrasonic intensity, frequency, and the distance between ultrasonic horn and the core. Sohrabi and Jamiolahmady (2009) evaluated the application of ultrasonic irradiation to well deliverability improvement in gas-condensate reservoirs. They performed experiments in the high-pressure glass micromodels and observed that a significant amount of condensate was mobilized and recovered by the application of ultrasound energy. Jin et al. (2012) used ultrasound in conjunction with thermochemical methods to enhance oil recovery from sludge. Their results showed that under optimum conditions, the oil content of sludge dropped from 43.13% to 1.01%. Keshavarzi et al. (2013) proposed a model to investigate the fluid percolation through fractured porous media under exposure to elastic waves. They found that at a constant pressure gradient, the amount of fluid percolation increased by increasing the wave amplitude.

According to the previous works, it is obvious that ultrasonic energy can considerably increase flow percolation through porous media, although, to the best of our knowledge, little attention has been paid to find a way to apply ultrasonic waves to the porous media on field scale in which the attenuation of the wave plays a significant role in the effects of waves on the flow of the fluid. According to Biot (1956), the attenuation of the wave in porous media is a function of fluid and rock properties and is inversely proportional to the square of the frequency.

In this study, a method is proposed to evaluate the attenuation factor of the ultrasonic wave radiated to a high permeable glass bead pack, as the porous medium, during a gravity drainage process.

2. Free fall gravity drainage

A schematic of the free fall gravity drainage process in which gas (as the non-wetting phase) pushes the oil (as the wetting phase) out of the cell is shown in Figure 1. It is assumed that there is an exact interface between oil and gas, which moves downward by the velocity of *u*. The velocity can be calculated with the application of Darcy equations for both phases.

$$u = \frac{\varnothing_{g1} - \varnothing_{gz}}{z} \times \frac{k_g}{\mu_g} \tag{1}$$

where, z is the distance between the oil-gas interface and the top of the cell. k_g and μ_g stand for the effective permeability and viscosity of the gas respectively; $\emptyset_{g1}$ and $\emptyset_{gz}$ represent flow potentials at the top of the cell and just above the interface in gas the phase respectively.

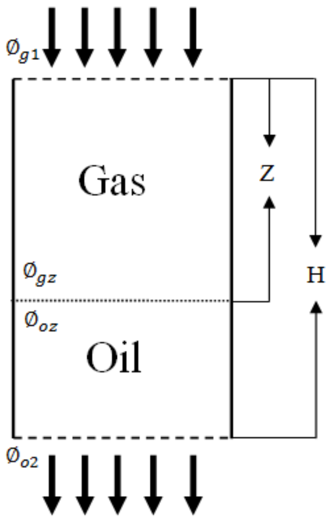

Figure 1
A schematic representation of the gravity drainage process.

$$u = \frac{\varnothing_{oz} - \varnothing_{o2}}{H - z} \times \frac{k_o}{\mu_o} \tag{2}$$

where, H is the height of the cell; k_o and μ_o denote the effective permeability and viscosity of the oil respectively; $\emptyset_{oz}$ and $\emptyset_{o2}$ represent flow potentials at just below the interface in the oil phase and at the bottom of the cell respectively. By combining these two equations, one may obtain:

$$\varnothing_{g1} - \varnothing_{gz} + \varnothing_{oz} - \varnothing_{o2} = uz\frac{\mu_g}{k_g} + u(H - z)\frac{\mu_o}{k_o} \tag{3}$$

Since the capillary pressure between two phases is $(\emptyset_{gz} - \emptyset_{oz})$, and capillary pressure at the exiting face is $(\emptyset_{g1} - \emptyset_{o2})$, one may obtain:

$$P_c^{'} - P_c + \Delta\rho g(H - z) = u\left(z\frac{\mu_g}{k_g} + (H - z)\frac{\mu_o}{k_o}\right) \tag{4}$$

where, P_c' is the capillary pressure at the end of the cell between gas and oil and could be considered negligible due to the capillary end effect (Van Golf-Racht, 1982); thus:

$$u = \frac{-P_c + \Delta\rho g(H - z)}{z\frac{\mu_g}{k_g} + (H - z)\frac{\mu_o}{k_o}} \tag{5}$$

where, $\Delta\rho = \rho_o - \rho_g$; by defining mobility ratio to be $M = \frac{\frac{k_g}{\mu_g}}{\frac{k_o}{\mu_o}}$ and considering the actual velocity in the porous medium as $u_{actual} = \frac{u}{\varphi}$, the following equation can be obtained:

$$u_{actual} = \frac{-P_c + \Delta\rho g(H - z)}{\varphi\frac{\mu_g}{k_g}\left(z + (H - z)M\right)} \tag{6}$$

In addition, the actual velocity is equal to the derivative of the interface location to time, i.e. $(u_{actual} = \frac{dz}{dt})$; therefore, one can have:

$$\frac{dz}{dt} = \frac{-P_c + \Delta\rho g(H - z)}{\varphi\frac{\mu_g}{k_g}\left(z + (H - z)M\right)} \tag{7}$$

2.1. Relative permeability of oil and gas phases

A Corey type approximation presented for drainage process is used to correlate relative permeabilities of both phases as follows:

$$k_{ro} = K_0^o\left(1 - S_g^*\right)^m \tag{8}$$

$$K_{rg} = K_0^g S_g^*\left(2 - S_g^*\right) \tag{9}$$

where, K_0^o, K_0^g, and m are the parameters of the Corey function with the default values of 1, 1, and 4 respectively; S_g^* stands for the normalized gas saturation as given bellow:

$$S_g^* = \frac{S_g}{1 - S_{wc}} \quad (10)$$

where, S_g is gas saturation and S_{wc} denotes the connate water saturation (Tarek Ahmed, 2000).

2.2. Measurement of capillary pressure

In a homogeneous, high permeable bead pack, it can be assumed that capillary pressure is constant during the experiment; moreover, due to the fact that at the end of the experiment capillary force equals the gravity force to stop oil drainage, the value of capillary pressure can be considered to be equivalent to the weight of the remaining fluid as reads:

$$Pc = \rho \times g \times \left(h - z_f\right) \quad (11)$$

where, z_f is the distance of the interface from the top of the cell at the end of the experiment.

3. Application of ultrasonic waves

3.1. Pressure amplitude

As a sound wave, ultrasound is transmitted through any substance, including solid, liquid, or gas, which possesses elastic properties. The movement of the vibrating body is communicated to the molecules of the medium, each of which transmits the motion to an adjoining molecule before returning to its original position (Mason et. al., 2002). For liquids and gases, particle oscillation takes place in the direction of the wave and produces longitudinal waves. Therefore, any molecule under the effect of waves oscillates around its original position. At any time (*t*), the displacement (*x*) of an individual molecule from its mean position is given by:

$$x = x_0 sin\omega t \quad (12)$$

where, x_0 is the displacement amplitude or maximum displacement of the particle and ω represents the angular frequency of the wave. The differentiation of the above equation leads to an expression for the particle velocity as given below:

$$v = v_0 cos\omega t \quad (13)$$

where, v_0 is the maximum velocity of the particle. In addition to the variation in the molecule position, when the sound wave travels through the fluid, there is a variation in pressure. At the point where the layers are crowded together (i.e. where the molecules are compressed), the pressure is higher than normal, whereas at the region where the layers are furthest apart (i.e. the rarefaction region) the pressure is lower than normal. As a result, the pressure (P_a) at any time is time- and frequency-dependent and can be described with the following equation:

$$P_a = P_A sin\omega t \quad (14)$$

where, P_A is the pressure amplitude (Mason et al., 2002).

3.2. Sound intensity

The particles of the medium were set into vibratory motion and thus possessed kinetic energy. This energy is derived from the wave itself. Using this principle, the energy (and hence intensity) associated with the applied ultrasonic field can be deduced. The kinetic energy per unit volume or the energy density (E) is given by:

$$E = \frac{1}{2}\rho v^2 \tag{15}$$

where, ρ is the density of the medium. If the sound energy passes through unit cross-sectional area with a velocity of *C*, then the volume swept out in unit time is *C* and the energy flowing in unit time is given by *EC*. Since the intensity (*I*) is defined as the amount of energy flowing per unit area per unit time for a plane progressive wave as given below,

$$I = EC = \frac{1}{2}\rho C v^2 \tag{16}$$

the particle velocity is related to acoustic pressure by (Wood, 1930):

$$P_A = v_0 \rho C \tag{17}$$

Thus by combining two previous equations a relationship between pressure amplitude and sound intensity is obtained as reads:

$$P_A^2 = 2\rho I C \tag{18}$$

Average energy applied to the system in half of the wave period is calculated by using the following expression:

$$E_m = \frac{1}{\frac{\pi}{\omega}} \int_0^{\frac{\pi}{\omega}} \frac{1}{2}\rho v^2 = \int_0^{\frac{\pi}{\omega}} \frac{1}{2}\rho v_0^2 \cos^2 \omega t = \frac{1}{4}\rho v_0^2 \tag{19}$$

By multiplying E_m with sound velocity C and combining it with Equation 17, average intensity is obtained:

$$I_m = \rho E_m = \frac{1}{4}\rho C v_0^2 = \frac{P_A^2}{2\rho C} \tag{20}$$

According to Equation 18, $\overline{P}_a^2 = 2\rho I_m C$; thus

$$\overline{P}_a = \frac{P_A}{\sqrt{2}} \tag{21}$$

This expression is the same as root mean square of the pressure wave.

3.3. Ultrasonic application in gravity drainage

In this work, it is assumed that ultrasonic energy causes an excess pressure gradient in the direction of the flow by adding acoustic pressure to the pressure gradient through the flow in Equation 5, the velocity of the interface between two phases is calculated by:

$$u = \frac{-P_c + \Delta\rho g\left(H - z\right) + \alpha \overline{P_a}}{\varphi \frac{\mu_g}{k_g}\left(z + \left(H - z\right)M\right)} \tag{22}$$

where, the parameter α is the attenuation factor which is dependent on the fluid and porous medium properties and is inversely proportional to the square of the wave frequency (Biot, 1956). Herein, attenuation factor is considered as a tuning parameter. By replacing $\overline{P_a}$ with its equivalence from Equation 21 and doing some manipulations previously mentioned for the case of free fall gravity drainage, one may obtain:

$$\frac{dz}{dt}=\frac{-P_c+\Delta\rho g\left(H-z\right)+\alpha\frac{P_A}{\sqrt{2}}}{\varphi\frac{\mu_g}{k_g}\left(z+\left(H-z\right)M\right)} \tag{23}$$

Two non-linear differential equations are described in Equations 7 and 23 as our final equations and should be solved in order to determine gas-oil interface versus time in the absence and presence of the ultrasonic radiation respectively.

4. Experimental set-up and procedure

The experimental setup includes a cylindrical cell made of Plexiglas with an outer diameter of 4 cm, a length of 30 cm, and an inner diameter of 3 cm, a graduated cylinder to measure the amount of extracted oil, and an ultrasonic wave generator with a frequency of 22 kHz, a nominal output power of 1000 watts, and an average effective power of 80 watts measured via accelerometer. The diameter of the ultrasonic horn is also 3 cm. A schematic representation of the experimental setup is shown in Figure 2. In this figure, ultrasonic energy passes through the air and is applied to the porous media from the top of the cell.

Before beginning the experiments, the apparatus was assembled and the glass beads were packed in the Plexiglas cylinder; one face of the cell is sealed and the other face is connected to the vacuum pump. The bead pack was first vacuumed to the desired pressure, where no other reduction was recorded and the gauge reading was stabilized, then the cell was fully saturated with the liquid sample and was placed in vertical gravity stable position. Porosity was measured by dividing imbibed fluid volume by the bulk volume. The experiments were conducted at ambient laboratory temperature, while the faces of the bead pack were opened to the atmospheric pressure. The experiments were conducted in two different conditions, namely in the presence and absence of ultrasonic waves, and the amount of oil recovery was measured in both conditions.

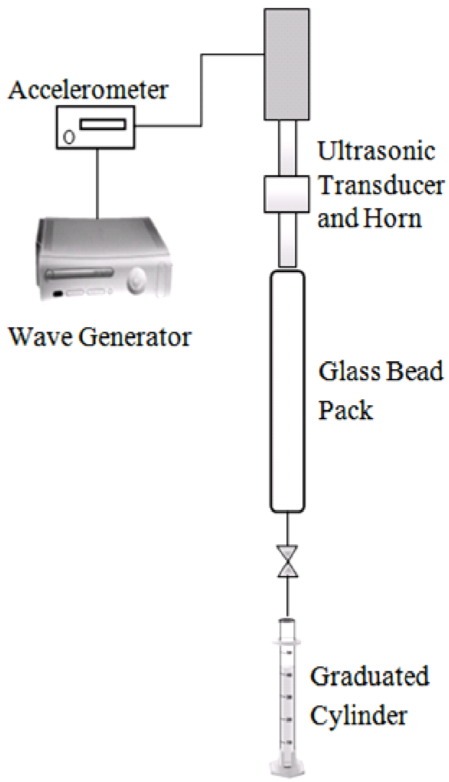

Figure 2
A schematic representation of the experimental setup.

The average grain size of the glass beads was 150-200 µm. To measure the absolute permeability of the bead pack, a constant height of liquid was placed at the top of the cell to ensure constant pressure gradient through the cell and the rate of the leaving fluid was measured; then, by applying Darcy equation, absolute permeability was computed. The porosity of porous media was measured to be 0.365 and the permeability was 34 Darcy. Air was used as the gas (non-wet) phase and Dorud oil sample and kerosene were used as the wetting phase. The viscosity of the fluids was measured using a rotary viscometer and the density was determined by measuring the weight of a certain amount of the fluid using a precision balance. Some properties of the experimental fluids are shown in Table 1.

Table 1
Properties of the experimental fluids.

Property	$\boldsymbol{\rho\ (\frac{kg}{m^3})}$	$\boldsymbol{\mu\ (pa.s)}$
Gas	1.25	0.000018
Dorud oil	860	0.0065
Kerosene	739	0.0009

5. Results and discussion

Ultimate values of the oil recovery for the non-sonicated case of Dorud crude oil and kerosene are 0.35 and 0.50 respectively; therefore, the values of z_f used in Equation 11 are determined to be 0.1050 m and 0.15 m respectively. Hence capillary pressures for both cases are calculated to be 1643.5 pa and 1108.5 pa respectively. The output power of the instrument is 80 watts, and thus the intensity of the wave is calculated by dividing output power by the area of the horn, and equals $1.13\times10^5\ \frac{watt}{m^2}$; therefore, the amplitude of the pressure wave is calculated by Equation 18 to be 9.65×10^3 pa. It should be noted that pressure wave is firstly generated in the air and is then applied to the porous medium. Equation 7 is solved numerically using Runge-Kutta of order 4 (ODE45 function in Matlab software package), knowing that z is equal to zero in the initial state. Next, by dividing values of z by the height of the cell H, recovery values are obtained. Recovery values obtained numerically are plotted together with the experimental data and, by changing the constants of relative permeability function, numerical results are matched to the experimental. Afterward, the matched data for relative permeability are used in the case of sonicated drainage. Equation 23 is solved using Runge-Kutta of order 4, the numerical results are plotted together with the experimental data, and then the value of attenuation parameter is changed until the numerical and experimental data are in reasonable agreement.

Values of recovery in the absence of ultrasonic waves are shown in Figures 3 and 5. As can be seen, the experimental data and numerical results are in good agreement. Furthermore, for the case with ultrasonic exposure, the amounts of oil recovery are depicted in Figures 4 and 6. The optimized values of α for Dorud crude oil and kerosene are determined to be 0.058 and 0.033 respectively. These low values of attenuation factor show that only a low percentage of pressure gradient is applied to the fluid.

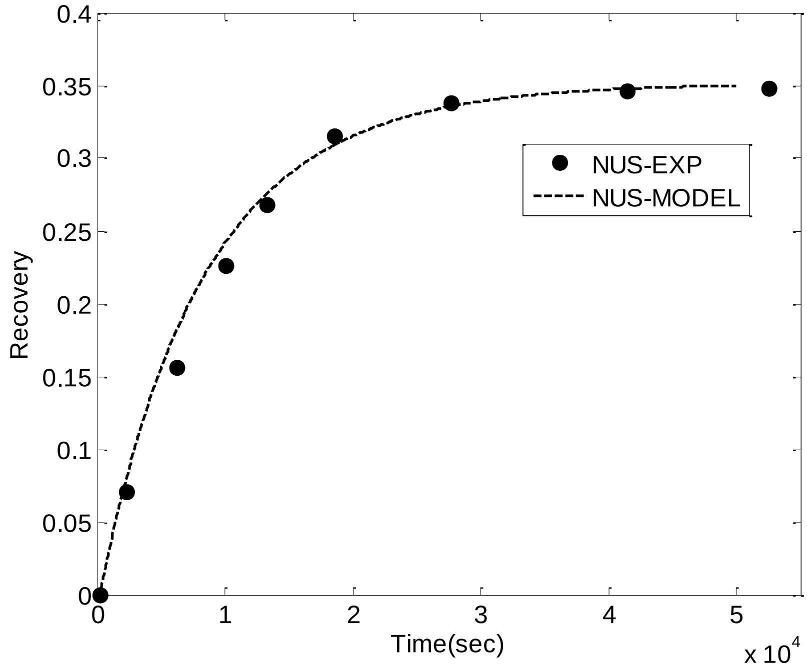

Figure 3
Recovery vs. time in the absence of ultrasonic waves (Dorud oil sample).

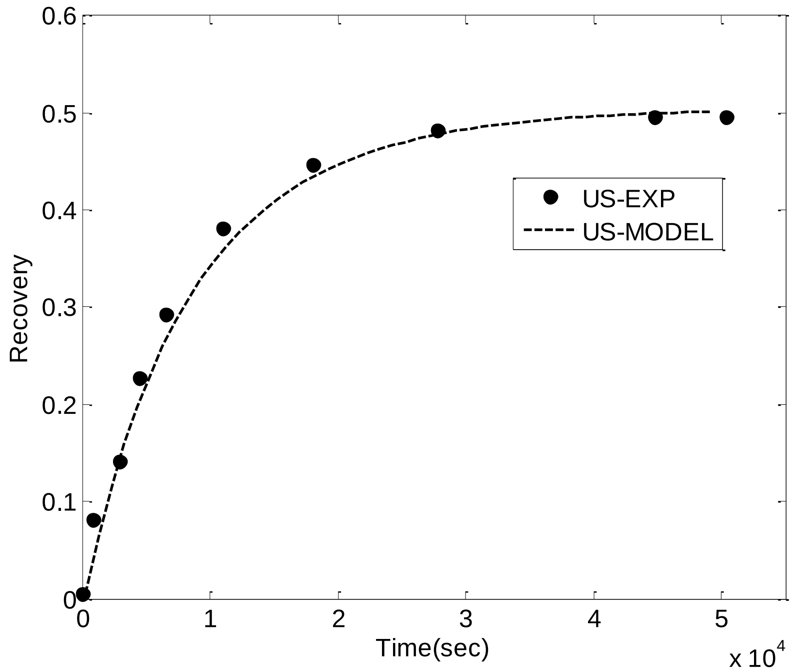

Figure 4
Recovery vs. time in the presence of ultrasonic waves (Dorud oil sample).

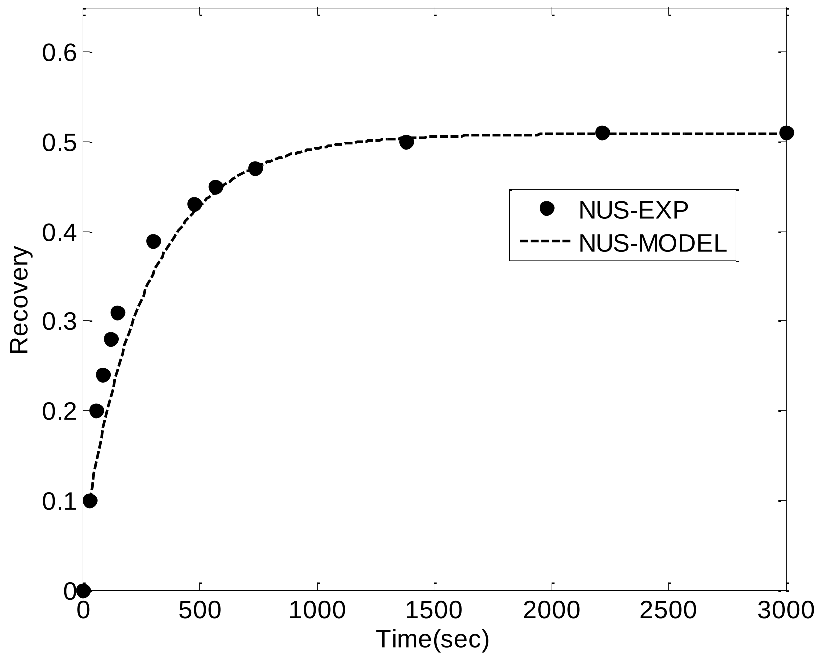

Figure 5
Recovery vs. time in the absence of ultrasonic waves (kerosene).

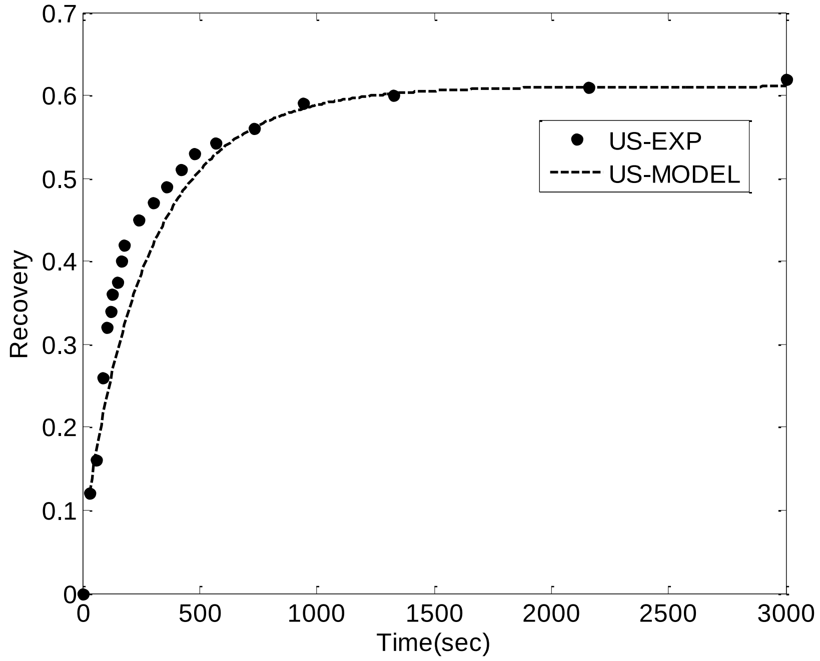

Figure 6
Recovery vs. time in the presence of ultrasonic waves (kerosene).

6. Conclusions

In the current study, a Corey type approximation was used for calculating relative permeabilities of wetting and non-wetting phases, and a piston-like displacement method was employed to predict the values of recovery for a gravity drainage process. The constants of Corey function were firstly found by matching the model to non-ultrasonic oil recovery data, and then the tuned relative permeabilities were used in the sonicated case in which the data were matched to the experimental data by changing the attenuation factor as the tuning parameter. The ultrasound attenuation factor was calculated for two different cases. In both cases, the results revealed that the sound attenuation, when being applied to porous media, was very high; moreover, only a small percentage of the pressure gradient caused by sound contributed to the flow, although a high percentage of recovery enhancement under the influence of ultrasonic energy was observed. Therefore, it can be claimed that ultrasonic waves have a very prominent effect on the enhancement of oil recovery. This work also gives us a hint that one of the effective ways to increase the efficiency of the ultrasonic waves is to increase the attenuation factor of the wave through porous media. Maybe a series of experiments evaluating the effects of wave frequency and intensity on different kinds of rock and fluid properties can help to find an optimum condition for using ultrasound. The parameter of attenuation factor can also be used in the commercial simulators to better predict the influence of ultrasonic waves on flow enhancement in porous media.

Nomenclature

E	: Sound wave energy density	$[M/LT^2]$
E_m	: Average energy in the half period of sound wave	$[M/LT^2]$
C	: Sound velocity	$[L/T]$
I	: Sound intensity	$[M/T^3]$
I_m	: Average sound intensity	$[M/T^3]$
H	: Height of the porous media	$[L]$
k	: Effective permeability	$[L^2]$
k_r	: Relative permeability	[-]
M	: Mobility ratio	[-]
m	: Corey equation exponent	[-]
p	: Pressure	$[M/LT^2]$
p_c	: Capillary pressure	$[M/LT^2]$
p_c'	: Capillary pressure at the end of core	$[M/LT^2]$
$\overline{p_a}$	: Root mean square of the pressure wave	$[M/LT^2]$
p_A	: Pressure amplitude	$[M/LT^2]$
PV	: Pore volume	$[L^3]$
p_c	: Capillary pressure	$[M/LT^2]$
Q	: Flow rate	$[L^3/T]$
Q_{act}	: Actual flow rate	$[L^3/T]$
q_t	: Production rate	$[L^3/T]$
Q_o	: Oil flow rate	$[L^3/T]$
R	: Radius of the sand pack	$[L]$
S	: Saturation	[-]
x	: Displacement	[L]
v	: Particle velocity	$[L/T]$
S_{wc}	: Connate water saturation	[-]
t	: Time	$[T]$
u	: Fluid velocity	$[L/T]$

z	: Displacement	[L]
Greeks		
μ	: Viscosity	$[M/LT]$
ρ	: Density	$[M/L^3]$
$\propto$	: Attenuation factor	[-]
φ	: Porosity	[-]
ω	: Angular frequency	[1/T]
$\emptyset$	: Fluid potential	$[M/LT^2]$
Subscripts		
g	: Gas	
o	: Oil	

Reference

Beresnev, I. A., Johnson, P.A., Elastic-wave Stimulation of Oil Production; a Review of Methods and Results, Geophysics 59, p. 1000-1017, 1994.

Biot, M .A., “Theory of Propagation of Elastic Waves in a Fluid-saturated Porous Solid. II. Higher Frequency Range”, the Journal of the Acoustical Society of America, Vol. 28 No. 2, p. 179-191, 1956.

Cherskiy, N., Tsarev, V., Konovalov, V., Kusnetsov, O., The Effect of Ultrasound on Permeability of Rocks to Water, Transactions (Doklady) of the USSR Academy of Sciences, Earth Science Section, Vol. 232.1, p. 201-204, 1977.

Duhon, R. D. and Campbel, J. M., “The Effect of Ultrasonic Energy on Flow through Porous Media”, SPE 1316, 2nd Annual Eastern Regional Meeting of SPE/AIME, Charleston, WV, 1965.

Hamida, T., Babadagli, T., Analysis of Capillary Interaction and Oil Recovery Under Ultrasonic Waves, Transport in Porous Media Vol. 70, p. 231-255, 2007.

Hamida, T., Babadagli, T., Displacement of Oil by Different Interfacial Tension Fluids Under Ultrasonic Waves, Colloids and Surfaces A, Physicochemical and Engineering Aspects, Vol. 316, p. 176-189, 2008.

Jin, Y., Zheng, X., Chu, X., Chi, Y., Yan, J., Cen, K., Oil Recovery from Oil Sludge through Combined Ultrasound and Thermochemical Cleaning Treatment, Industrial & Engineering Chemistry Research, Vol. 51, p. 9213-9217, 2012.

Keshavarzi, B., Karimi, R., Najafi, I., Ghazanfari, M., Amani, M., Ghotbi, C., Investigation of Low Frequency Elastic Wave Application for Fluid Flow Percolation Enhancement in Fractured Porous Media, Petroleum Science and Technology, Vol. 31, p. 1159-1167, 2013.

Mason T. J. and Lorimer J. P., “Applied Sonochemistry: Uses of Power Ultrasound in Chemistry and Processing”Wiley-VCH Verlag GmbH & Co. KGaA, ISBN: 3-527-30205-0, 2002.

Naderi, K. and babadagli, T., “Effect of Ultrasonic Intensity and Frequency on Oil/Heavy-oil Recovery from Different Wettability Rocks”,SPE/PS/CHOA, 117324, 2008.

Naderi, K., Babadagli, T., Influence of Intensity and Frequency of Ultrasonic Waves on Capillary Interaction and Oil Recovery from Different Rock Types. Ultrasonics Sonochemistry, Vol. 17, p. 500-508, 2010.

Sohrabi, M., Jamiolahmady, M., Application of Ultrasonic Irradiation for Well Deliverability Improvement in Gas-condensate Reservoirs, Journal of Petroleum Science and Engineering, Vol. 64, p. 88-94, 2009.

Tarek Akmed, “Reservoir Engineering Handbook”, Gulf Professional Publishing, 2nd Edition, 2000.

Van Golf-Racht T. D., “Fundamentals of Fractured Reservoir Engineering”, Elsievier Scientific Publishing Company, 1982.

Wood, A. B., A Textbook of Sound: Being an Account of the Physics of Vibrations with Special Reference to Recent Theoretical and Technical Developments. Macmillan, New York, 1941.